# Theoretically Based Algorithms for Robustly Tracking Intersection Curves of Deforming Surfaces ⋆

Xianming Chen [a] Richard F. Riesenfeld [a] Elaine Cohen [a]
James Damon [b]

[a] *School of Computing, University of Utah, Salt Lake City, UT 84112*

[b] *Department of Mathematics, University of North Carolina, Chapel Hill, NC 27599*

**Abstract**

This paper applies singularity theory of mappings of surfaces to 3-space and the generic transitions occurring in their deformations to develop algorithms for continuously and robustly tracking the intersection curves of two deforming parametric spline surfaces, when the deformation is represented as a family of generalized offset surfaces. The set of intersection curves of 2 deforming surfaces over all time is formulated as an implicit 2-manifold $\mathcal{I}$ in an augmented (by time domain) parametric space $\mathbb{R}^5$. Hyper-planes corresponding to some fixed time instants may *touch* $\mathcal{I}$ at some isolated transition points, which delineate transition events, i.e., the topological changes to the intersection curves. These transition points are the 0-dimensional solution to a rational system of 5 constraints in 5 variables, and can be computed efficiently and *robustly* with a rational constraint solver using subdivision and hyper-tangent bounding cones. The actual transition events are computed by contouring the local osculating paraboloids. Away from any transition points, the intersection curves do not change topology and evolve according to a simple evolution vector field that is constructed in the *Euclidean space* in which the surfaces are embedded.

*Key words:* Deforming Surface/Surface Intersection, Generalized Offset Surface, Evolution Vector Field, Topological Transition Event, Shape Computation of Implicit 2-Manifold in 5-Space

⋆ This work is supported in part by NSF CCR-0310705, NSF IIS-0218809, NSF CCR-0310546, and NSF DMS-0405947. All opinions, findings, conclusions or recommendations expressed in this document are those of the authors and do not necessarily reflect the views of the sponsoring agencies.

*Email address:* xchen@cs.utah.edu (Xianming Chen).

*URL:* http://www.cs.utah.edu/∼xchen/ (Xianming Chen).

## 1 Introduction and Related Work

In this paper, we consider the dynamically changing intersection of two deforming parametric surfaces. The surface deformations are represented by families of generalized offset surfaces, which are examples of "radial flows" of generalized offset vector fields introduced in [6, 7] (also see [8] for a mathematically less technical discussion). This extends the standard unit normal offset surfaces. Specifically, let $\varsigma(s)$, $s \in \mathbb{R}^2$, be a parametrization of an initial regular surface $M$. A generalized offset vector field $U(s)$ on $M$ is a vector field $U(s)$ defined on $M$ which is not tangent to $M$ at any point, and need not have unit-length nor be orthogonal to the tangent plane of $M$. The generalized offset surface flow is defined by,

$$\sigma(s,t) = \varsigma(s) + tU(s); \tag{1}$$

where $0 \leq t \leq 1$ is the offset time. Each of the two deforming surfaces is assumed to remain regular and be free of self-intersections throughout the deformation process. Conditions ensuring such regularity are given in [6] and [8].

Research into finding surface-surface intersections has mostly focused on the static problem [4, 16, 28, 34, 39], and the case of the unit normal offset surfaces [9, 11, 12, 18, 21, 23, 29, 37], We emphasize the topological robustness of surface intersection, which has been an important and extensively researched topic for static surface-surface intersection [2, 15, 20, 24, 25, 31, 32]. In [17], Jun et al. worked on surface slicing, i.e., the intersection of a surface with a series of parallel planes, exploring the relation between the transition points and the topology of contour curves. The transition points, though, are used only to efficiently and robustly find the starting point of the contour curves for a marching algorithm [3, 5] to trace out the whole curve. Ouyang et al. [27] applied a similar approach to the intersection of two unit normal vector offset surfaces.

Applied to mappings of surfaces to $\mathbb{R}^3$, singularity theory [1] provides a theoretical classification of both the local stable properties of mappings of surfaces and of the generic transitions they undergo under deformation. Our assumptions on the regularity of the surfaces characterizes the transition of the intersection curves of the deforming surfaces to one of a list of standard generic transitions. Between transitions, the intersection curves evolve in a smooth way without undergoing topological transitions.

This paper is organized to deal with these two cases. In Section 2, we construct an evolution vector field which allows us to follow the evolution of intersection curves by discretely solving a differential equation in the parametric space. In Section 3, we represent the locus of intersection curves of the two deforming surfaces as a 2–manifold $\mathcal{I}$ in a 5–dimensional *augmented parameter space*. In

Section 4 we turn to the second problem of computing the transition events, and tracking the topological changes of the intersection curves occurring at transition points. In Section 4.1, we enumerate the generic transition points classified by singularity theory and provide an alternative characterization as critical points of a function on the implicit surface $\mathcal{I}$. This provides the theoretical basis to our algorithm that detects transition points as the simultaneous 0-set of a rational system of 5 constraints in 5 variables. Then, in Section 4.2 we compute the transitions in the intersection curves using contours on the local osculating quadric of the surface $\mathcal{I}$ at the critical points. A concluding discussion of the issues ensues in Section 5.

## 2 Evolution of Intersection Curves

Consider two deforming surfaces, $\sigma$ and $\hat{\sigma}$, represented as generalized offset surfaces,

$$\sigma(s,t) = \varsigma(s) + t\ U(s),$$
$$\hat{\sigma}(\hat{s},t) = \hat{\varsigma}(\hat{s}) + t\ \hat{U}(\hat{s}),$$

where $s = (s_1, s_2) \in \mathbb{R}^2$ and $\hat{s} = (\hat{s}_1, \hat{s}_2) \in \mathbb{R}^2$ are the parameters of $\varsigma(s)$ and $\hat{\varsigma}(\hat{s})$, and their corresponding offset vector fields $U(s)$ and $\hat{U}(\hat{s})$, respectively. We write the coordinate representation of the deforming surfaces by

$$\sigma(s,t) = (x(s,t), y(s,t), z(s,t)) \text{ and } \hat{\sigma}(\hat{s},t) = (\hat{x}(\hat{s},t), \hat{y}(\hat{s},t), \hat{z}(\hat{s},t)).$$

We let $\mathcal{L}_0$ denote the set of the points in $\mathbb{R}^3$ which will lie on the intersection of the two deforming surfaces for at least one time $t$. Consider a point $P$ on an intersection curve of the two deforming surfaces at some time $t$. We first assume that the tangent planes to the two offset surfaces at $P$ are different; otherwise, we are in the singular case corresponding to a transition event, which we will discuss in section 4. We use the notation $\sigma_i = (x_i, y_i, z_i)$ to denote the partial derivative $\frac{\partial \sigma}{\partial s_i} = (\frac{\partial x}{\partial s_i}, \frac{\partial y}{\partial s_i}, \frac{\partial z}{\partial s_i})$ $(i = 1, 2)$, and analogously for $\hat{\sigma}_i$. Define

$$N = \sigma_1 \times \sigma_2, \quad \hat{N} = \hat{\sigma}_1 \times \hat{\sigma}_2$$

to be the 2 non-unit length normals to each of the two surfaces, respectively. Further let

$$\bar{N} = (N \times \hat{N}) \times \hat{N}.$$

to be the tangent vector of $\hat{\sigma}$ at $P$ that is perpendicular to the intersection curve.

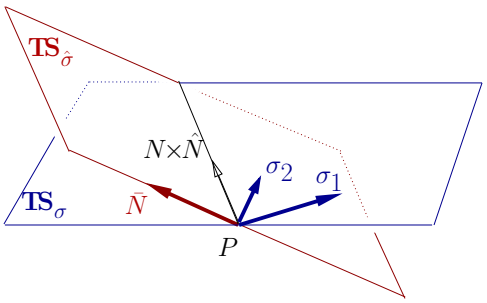


Fig. 1. **Local Basis** $\{\sigma_1, \sigma_2, \bar{N}\}$

Because the two tangent planes to the two surfaces at $P$ are different, $\{\sigma_1, \sigma_2, \bar{N}\}$ is a basis of $\mathbb{R}^3$ (Fig. 1). Decomposing $\delta U = \hat{U} - U$ in this basis gives,

$$\delta U = \hat{U} - U = a\sigma_1 + b\sigma_2 + c\bar{N}$$

Because the last term $c\bar{N}$ lives entirely in the tangent plane to the surface $\hat{\sigma}$ at $P$, it has a decomposition relative to the basis $\{\hat{\sigma}_1, \hat{\sigma}_2\}$,

$$-c\bar{N} \;=\; \hat{a}\hat{\sigma}_1 + \hat{b}\hat{\sigma}_2,$$

Thus, we have

$$\delta U \;=\; \hat{U} - U \;=\; a\sigma_1 + b\sigma_2 + (-\hat{a}\hat{\sigma}_1 - \hat{b}\hat{\sigma}_2),$$

or,

$$\hat{U} + (\hat{a}\hat{\sigma}_1 + \hat{b}\hat{\sigma}_2) \;=\; U + a\sigma_1 + b\sigma_2$$

Consequently, we have the **evolution vector field** with two equivalent representations (over two different basis of $\mathbb{R}^3$),

$$\eta = U + a\sigma_1 + b\sigma_2 \tag{2}$$

$$\hat{\eta} = \hat{U} + \hat{a}\hat{\sigma}_1 + \hat{b}\hat{\sigma}_2 \tag{3}$$

This vector field is defined on a neighborhood of the point $P$ in $\mathbb{R}^3$, rather than just on the surfaces.

Next, for any point $P$ which lies on a curve of intersection for the deforming surfaces, we can define a scalar field $\phi$ in a neighborhood of $P$ (in $\mathbb{R}^3$). By the inverse function theorem, there is a neighborhood of $P$ which is entirely covered by each deforming family. For a point $P'$ in this neighborhood, we define $\phi(P') = \hat{t} - t$, where $\hat{t}$ (resp. $t$) is the time when the surface $\hat{\sigma}(\hat{s}, t)$ (resp. $\sigma(s, t)$) reaches $P'$. Although $\phi$ is not defined everywhere on $\mathbb{R}^3$, it is defined on a neighborhood of $\mathcal{L}_0$.

The following properties involving $\phi$, $\eta$, and $\mathcal{L}_0$ can be shown to hold:

(1) The directional derivative $\frac{\partial \phi}{\partial \eta} = 0$ identically wherever $\phi$ is defined. This

is readily verified by directly computing the directional derivative of $\phi$ with respect to $\eta$.

(2) The zero level set of $\phi$ is exactly $\mathcal{L}_0$.

(3) Hence, $\eta$ is tangent to $\mathcal{L}_0$ at all points.

Now suppose point $P$ is on $\mathcal{L}_0$, and lies on an intersection curve at time $t$. The condition that $\eta$ is tangent to $\mathcal{L}_0$ allows us to follow the evolution of $P$ on future intersection curves by solving the differential equation

$$\frac{d\gamma}{dt} = \eta(\gamma) \quad \text{with initial condition } \gamma(0) = P$$

for $\gamma(t) \in \mathbb{R}^3$. The evolution vector field $\eta$ is the image of the vector field $\xi = \frac{\partial}{\partial t} + a\frac{\partial}{\partial s_1} + b\frac{\partial}{\partial s_2}$ under the parametrization map $\sigma$. Thus, the evolution could likewise be followed on the parameter space using instead the vector field $\xi$, and analogously for $\hat{\sigma}$.

Then, we can use a discrete algorithm for solving the differential equations to follow the evolution of the intersection curves over a time interval void of transitions. Specifically, for small time $dt$, $P$ moves to $Q = P + dt\ (U + a\sigma_1 + b\sigma_2)$ on the physical surface, and if $p = s \in \mathbb{R}^2$ corresponds to $P$, then $q = s + (a\ dt, b\ dt)$ will correspond to $Q$ in the parameter space, and analogously for $\hat{\sigma}$. The first order marching algorithm accumulates error over time, so point correction can be used to increase the quality. Various point correction algorithms are discussed in [5] in the context of static surface-surface intersection. We have adopted the middle point algorithm as presented in [4] to relax the points onto the actual intersection curve. As the evolution proceeds, sample points for the intersection curves are adaptively inserted or deleted so that the spacing of two consecutive sample points is neither too far away nor too close, and so that the angle deviation of 3 consecutive sample points stays small.

## 3 Formulation in the Augmented Parametric Space

Define a vector distance mapping

$$d(s, \hat{s}, t) = \hat{\sigma} - \sigma : \mathbb{R}^5_{\{s,\hat{s},t\}} \longrightarrow \mathbb{R}^3 \tag{4}$$

where $\mathbb{R}^5_{\{s,\hat{s},t\}}$ [1] is the combined parametric space of the two surfaces and the time domain, and is thus called **augmented parametric space**. The canonical orthonormal basis $\mathbb{R}^5_{\{s,\hat{s},t\}}$ is denoted as $\{e_{s_1}, e_{s_2}, e_{\hat{s}_1}, e_{\hat{s}_2}, e_t\}$. The 0-set of

[1] $\mathbb{R}^5_{\{s,\hat{s},t\}}$ denotes $\mathbb{R}^5$ with the five coordinates being $s_1, s_2, \hat{s}_1, \hat{s}_2, t$ and analogously, for $\mathbb{R}^3_{\{s,t\}}$, etc.

this mapping, denoted $\mathcal{I}$ hereafter in this paper, gives the set of all intersection points in $\mathbb{R}^5_{\{s,\hat{s},t\}}$. Note that $d(s,\hat{s},t)$ concisely represents related equations for three separate coordinate functions. Considering the $x$-component $d_x(s,\hat{s},t)$. $d_x(s,\hat{s},t)=0$ defines a hyper-surface in $\mathbb{R}^5_{\{s,\hat{s},t\}}$, with corresponding normal

$$N_x = \nabla d_x = (-x_1, \ -x_2, \ \hat{x}_1, \ \hat{x}_2, \ \delta U_x) \tag{5}$$

The component functions $y$ and $z$ define another two hyper-surfaces with analogous expressions for their normals $N_y$ and $N_z$. Geometrically, $\mathcal{I}$ is the locus of intersection points of these three hyper-surfaces in $\mathbb{R}^5_{\{s,\hat{s},t\}}$. The Jacobian [22] of the mapping $d(s,\hat{s},t):\mathbb{R}^5_{\{s,\hat{s},t\}} \longrightarrow \mathbb{R}^3$ is,

$$\mathcal{J} = (N_x \ N_y \ N_z)^t = \begin{pmatrix} -x_1 & -x_2 & \hat{x}_1 & \hat{x}_2 & \delta U_x \\ -y_1 & -y_2 & \hat{y}_1 & \hat{y}_2 & \delta U_y \\ -z_1 & -z_2 & \hat{z}_1 & \hat{z}_2 & \delta U_z \end{pmatrix} = (-\sigma_1 \ \ -\sigma_2 \ \ \hat{\sigma}_1 \ \ \hat{\sigma}_2 \ \ \delta U). \tag{6}$$

**Remark 1** If the two tangent planes to the two deforming surfaces at the intersection point are not the same, then both of the triple scalar products (determinants) $[\sigma_1\sigma_2\hat{\sigma}_i]$'s $(i=1,2)$ can not simultaneously vanish, and so $\mathcal{J}$ has the full rank of 3. Otherwise, the two tangent planes must be the same. Assuming, at such a touching point, $\delta U$ is not on the common tangent plane, i.e., $[\hat{\sigma}_1\hat{\sigma}_2\delta U] \neq 0$ and $[\sigma_1\sigma_2\delta U] \neq 0$, $\mathcal{J}$ again has the full rank. Therefore, the 0-set of the distance mapping $d(s,\hat{s},t) = \hat{\sigma} - \sigma : \mathbb{R}^5_{\{s,\hat{s},t\}} \longrightarrow \mathbb{R}^3$, is a well defined implicit 2-manifold in the augmented parametric space.

## 4 Transition of Intersection Loops

In singularity theory, the situation we consider is considered generic. That is, except for a finite set of times, the two closed surfaces intersect transversely, that is, at each intersection point the tangent planes of the surfaces are different. Thus, the method presented in Section 2 can be applied to track the evolution of the curves. Over such time intervals topological changes are guaranteed not to occur.

At the remaining finite number of times, there will be intersection points at which the tangent planes coincide (non-transverse points). Again for *generic deformations*, singularity theory describes exactly the transitions in intersection curves that can occur as the evolution passes such times. These transitions can always be given (up to a change of coordinates) by standard model equations, so there is essentially a unique way for each transition to occur. We shall refer to points (and times) at which transitions occur as *transition points*. These transitions are classified as,

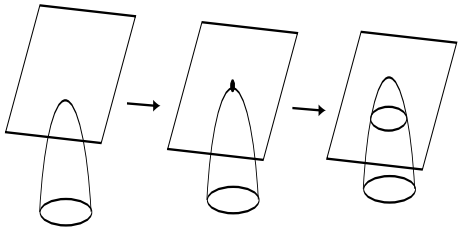

Fig. 2. **Creation of Intersection Curve Component**

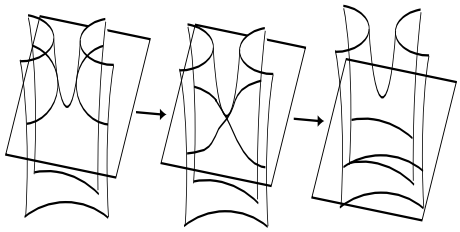

Fig. 3. **Exchange of Intersection Curve Components**

(1) *a creation event*, when a new intersection loop is created (Fig. 2),
(2) *an annihilation event*, when one of the current loops collapses and disappears (Fig. 2 in the reverse direction),
(3) *an exchange event*, when two branches of intersection curves meet and exchange branches (Fig. 3).

The exchange event can have two different global consequences. If the two branches are part of the same curve, an intersection loop is split into two loops and we refer to this as a *splitting event* (Fig. 6). If the branches are from distinct intersection loops, a single loop is formed in a *merge event* (Fig. 6 in reverse order).

### *4.1 Detection of Transition Events*

In this sub-section, we formulate the topological transition points as the 0-set of a rational system of 5 nonlinear constraints in 5 variables. The 0-set has dimension 0, i.e., it is a discrete collection of points. It can be *robustly and efficiently* computed using a rational constraint solver [10, 33]. The robustness is achieved by bounding the subdivided implicit surface $\mathcal{I}$ with the corresponding hyper-tangent cone [10], an extension of the bounding tangent cones for explicit plane curves and explicit surfaces [31, 32].

Let us recall that the implicit 2-manifold $\mathcal{I}$ in $\mathbb{R}^5_{\{s,\hat{s},t\}}$ is the locus of intersection points of the two deforming surfaces, over the whole time period. Geometrically, the intersection curves, at some time point, are the corresponding height contour of $\mathcal{I}$ when the $t$ is regarded as the vertical axis. By Remark 1, $\mathcal{I}$ is

a well-defined 2-manifold, and as a consequence of the generic forms for the transition points, the height function $t$ has only non-degenerate critical points which are of the three types: upward elliptic points, downward elliptic points, and hyperbolic (saddle) points (cf. Fig. 4). Therefore, it is obvious that there will be one of the three transition events listed earlier, if the tangent space to $\mathcal{I}$ at a point $(s, \hat{s}, t)$ is orthogonal to the $t$-axis. Since $\mathcal{I}$ and its tangent space have the same dimension, namely, 2, the orthogonality condition is tantamount to satisfying two equations,

$$T_1 \cdot e_t = 0, \qquad T_2 \cdot e_t = 0,$$

where $T_1$ and $T_2$ are any two vectors spanning the tangent space. A simple and natural way to construct such a pair of tangent vectors is to let $T_1$ be the tangent to an $s_2$-iso-curve on $\mathcal{I}$ with the extra constraint $s_2 = c_2$ for some constant $c_2$, and let $T_2$ be the tangent to an $s_1$-iso-curve on $\mathcal{I}$ with the extra constant $s_1 = c_1$ for some constant $c_1$. Noticing that an $s_2$-iso-curve is the intersection of 4 hyper surfaces in $\mathbb{R}^5_{\{s,\hat{s},t\}}$, defined by $s_2 = c_2$, $d_x = 0$, $d_y = 0$, and $d_z = 0$,

$$T_1 = \begin{vmatrix} e_{s_1} & e_{s_2} & e_{\hat{s}_1} & e_{\hat{s}_2} & e_t \\ 0 & 1 & 0 & 0 & 0 \\ -x_1 & -x_2 & \hat{x}_1 & \hat{x}_2 & \delta U_x \\ -y_1 & -y_2 & \hat{y}_1 & \hat{y}_2 & \delta U_y \\ -z_1 & -z_2 & \hat{z}_1 & \hat{z}_2 & \delta U_z \end{vmatrix} = (\mathscr{T}^{\hat{1}\hat{2}\delta},\ 0,\quad \mathscr{T}^{1\hat{2}\delta},\quad -\mathscr{T}^{1\hat{1}\delta},\quad \mathscr{T}^{1\hat{1}\hat{2}}),$$

where $\mathscr{T}$' denotes the triple scalar product of its 3 corresponding vectors indicated by the superscripts. Superscripts $i$ and $\hat{i}$ represent $\sigma_i$ and $\hat{\sigma}_i$, respectively, while a superscript $\delta$ represents $\delta U$ (e.g., $\mathscr{T}^{\hat{1}\hat{2}\delta} = [\hat{\sigma}_1\ \hat{\sigma}_2\ \delta U]$). A similar derivation exists for $T_2$. Thus, we have in general

$$T_i = \mathscr{T}^{\hat{1}\hat{2}\delta}\ e_{s_i} + \mathscr{T}^{i\hat{2}\delta}\ e_{\hat{s}_1} - \mathscr{T}^{i\hat{1}\delta}\ e_{\hat{s}_2} + \mathscr{T}^{i\hat{1}\hat{2}}\ e_t, \quad i = 1, 2. \tag{7}$$

At transition points, the last component of $T_1$ and $T_2$ vanishes, i.e.

$$T_1 \cdot e_t = \mathscr{T}^{1\hat{1}\hat{2}} = [\sigma_1\ \hat{\sigma}_1\ \hat{\sigma}_2] = 0, \quad T_2 \cdot e_t = \mathscr{T}^{2\hat{1}\hat{2}} = [\sigma_2\ \hat{\sigma}_1\ \hat{\sigma}_2] = 0, \tag{8}$$

**Remark 2** At a transition point, $T_1$ and $T_2$ are guaranteed to be independent of each other because, by Eq. (7), the $s_1$ coordinate component of $T_2$ vanishes while the corresponding component of $T_1$ is non-zero (cf. Remark (1) as well). It is also easily seen that Eq. (8) simply requires the two tangents $\sigma_1$ and $\sigma_2$ to the first offset surface to be perpendicular to the normal of the second offset surface, i.e., the two tangent planes to the two deforming surfaces in the euclidean space are coincident.

Finally, together with $\hat{\sigma} - \sigma = 0$, Eq. (8) gives a rational system with 5 constraints in 5 variables, whose 0-dimensional solution set contains all the transition points we are seeking.

### *4.2 Compute the Structural Change at Transition Events*

In this section, we perform the shape computation of the 2-manifold $\mathcal{I}$ at a transition point, and subsequently compute the corresponding transition event by contouring the osculating paraboloid [19, 26] to the local shape (Fig. 4).

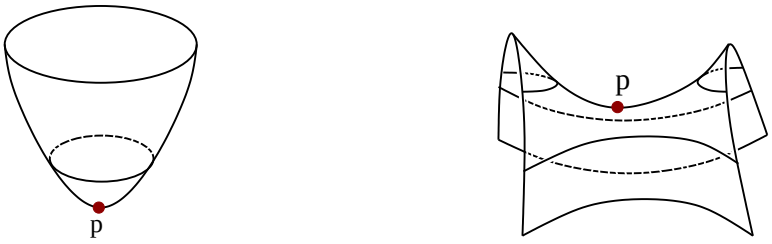


(a) elliptic (b) hyperbolic

Fig. 4. **Contour Osculating Paraboloid**

The implicit surface $\mathcal{I}$ is a 2-manifold in a 5-space $\mathbb{R}^5_{\{s,\hat{s},t\}}$. Shape computation is difficult because it is an implicit surface, and also because its codimension $\neq 1$.

Most recently, a comprehensive set of formulas for curvature computation on implicit curves/surfaces with further references were presented in [13]. However, it is limited to curves/surfaces embedded in $2D$ or $3D$ spaces. There exists some literature from the visualization community, e.g., [14, 36] and references therein, that develops second order derivative computation on iso-surfaces extracted from trivariate functions. Most of these approaches use discrete approximations. Recently, [35] developed B-spline representations for the Gaussian curvature and squared mean curvature of the iso-surfaces extracted from volumetric data defined as a trivariate B-spline function, and subsequently presented an exact curvature computation for every possible point of the 3D domain. While we seek an exact differential computation, the task here significantly differs from that in [35] and [14, 36] since the implicit 2-manifold $\mathcal{I}$ has codimension 3. In [38], a set of formulas for computing Riemannian curvature, mean curvature vector, and principal curvatures, specifically for a 2-manifold, and with *arbitrary* codimension, is presented. The specific 2nd order problem we seek to solve, namely initializing the newly created intersection loop, or switching the two pairs of hyperbolic-like segments, is based on *shape approximation*. For a surface in 3-space, the local shape approximation is

simply the osculating quadric, expressed in the second fundamental form [26] as $z = \frac{1}{2}II(a, a)$ where $a$ is any tangent vector, and $z$ is the vertical distance from the local surface point to the tangent plane. Observing that the second order shape approximation is best done if the codimension is 1, we do not compute the second fundamental form directly on the 2-manifold in 5-space. Instead, we project the 2-manifold to a 3-space of either $\mathbb{R}^3_{\{s,t\}}$ (our choice in this paper) or $\mathbb{R}^3_{\{\hat{s},t\}}$. The second fundamental form is then computed for this projected 2-manifold, and shape approximation is achieved subsequently. Notice that the shape approximation in the projected 3-space gives only a partial answer to the transition event; the full solution is achieved by the tangential mapping between the projected 2-manifold and the original one (cf. Observation 1 below).

#### *4.2.1 Projection of $\mathcal{I}$ to $\mathbb{R}^3_{\{s,t\}}$*

Near a critical point, $T_1$ and $T_2$ (cf. Eq. (7)) give two vectors spanning (cf. Remark 2) the tangent space to $\mathcal{I}$. By projecting $\mathcal{I}$ onto $R^3_{\{s_1,s_2,t\}}$ and ignoring the $\hat{s}_1$ and $\hat{s}_2$ components, we transform $\mathcal{I}$, a 2-manifold in $\mathbb{R}^5_{\{s,\hat{s},t\}}$, into a surface in $R^3_{\{s,t\}}$, denoted as $\mathcal{I}^s$. Furthermore, $T_1$ and $T_2$ are projected to

$$T_1^s = \mathscr{T}^{\hat{1}\hat{2}\delta}\, e_{s_1} + \mathscr{T}^{1\hat{1}\hat{2}}\, e_t, \quad T_2^s = \mathscr{T}^{\hat{1}\hat{2}\delta}\, e_{s_2} + \mathscr{T}^{2\hat{1}\hat{2}}\, e_t, \tag{9}$$

where we have used the superscript $s$ to distinguish the tangents from their counterparts of $\mathcal{I}$ in the original augmented parametric space $\mathbb{R}^5_{\{s,\hat{s},t\}}$.

Exactly at the transition point where $\mathscr{T}^{1\hat{1}\hat{2}} = \mathscr{T}^{2\hat{1}\hat{2}} = 0$ (cf. Eq. (8)), we have,

$$T_1^s = \mathscr{T}^{\hat{1}\hat{2}\delta}\, e_{s_1}, \quad T_2^s = \mathscr{T}^{\hat{1}\hat{2}\delta}\, e_{s_2}.$$

Hereafter, a point in the tangent space $\mathbf{TS}_{\mathcal{I}^s}$ is typically specified by its 2 coordinates, say, $a_1$ and $a_2$, with respect to the basis $\{T_1^s, T_2^s\}$, the canonical frame $\{e_{s_1}, e_{s_2}\}$ scaled by $\mathscr{T}^{\hat{1}\hat{2}\delta}$.

Notice that, $T_1$ and $T_2$ span the tangent space to $\mathcal{I}$ in the 5-space $R^5_{\{s_1,s_2,\hat{s}_1,\hat{s}_2,t\}}$, while their projection $T_1^s$ and $T_2^s$ span the tangent space to $\mathcal{I}^s$ in the 3-space $R^3_{\{s_1,s_2,t\}}$. Therefore, the projection, denoted as $\pi$ hereafter, is a diffeomorphism.

**Observation 1** *At a transition point, the inverse of the derivative of $\pi$ maps (cf. Eqs. (7)),*

$$(1,0) \mapsto (\mathscr{T}^{\hat{1}\hat{2}\delta}, 0, \mathscr{T}^{1\hat{2}\delta}, -\mathscr{T}^{1\hat{1}\delta}, 0), \qquad (0,1) \mapsto (0, \mathscr{T}^{\hat{1}\hat{2}\delta}, \mathscr{T}^{2\hat{2}\delta}, -\mathscr{T}^{2\hat{1}\delta}, 0),$$

*where $(1,0)$ and $(0,1)$ are the coordinates of two points in the local tangent space $\mathbf{TS}_{\mathcal{I}^s}$ with basis $\{T_1^s, T_2^s\}$.*

*4.2.2 The Shape Computation*

The local shape of $\mathcal{I}^s$ in $\mathbb{R}^3_{\{s,t\}}$ is determined from the second fundamental form $II$.

Typically, $II$ of any *parameterized* surface is represented in a matrix form involving the $2^{nd}$ order partial derivatives of the surface with respect to its parameters. Even though, the surface $\mathcal{I}^s$ we are considering is implicitly defined rather than being given by a parametric representation, it does have two independent tangent vector fields, $T_1^s$ and $T_2^s$, on a neighborhood of any transition point. Moreover, $II$ can be computed by covariant derivatives [26] on the tangent vector fields; specifically, at *a transition point*, the matrix of the second fundamental form in the $\{T_1^s, T_2^s\}$ basis, denoted as $\mathcal{L}$, is

$$\mathcal{L} = \Big(N^s \cdot \nabla_{T_i^s} T_j^s\Big) = \Big(\nabla_{T_i^s} T_j^s \cdot e_t\Big), \tag{10}$$

and the local shape is approximated by the osculating quadric [26, 19],

$$\delta t = \frac{1}{2} II(a,a) = \frac{1}{2} \begin{pmatrix} a_1 & a_2 \end{pmatrix} \mathcal{L} \begin{pmatrix} a_1 \\ a_2 \end{pmatrix}, \tag{11}$$

where $a = (a_1, a_2) \in \mathbf{TS}_{\mathcal{I}^s}$. Notice that we wrote the left hand side as $\delta t$, because, at a transition point, the tangent plane $\mathbf{TS}_{\mathcal{I}^s}$ is horizontal, and thus the local vertical height is exactly the time deviation from the considered transition point.

We compute the second fundamental form II for the surface $\mathcal{I}^s$ in $\mathbb{R}^3$ at a transition point by computing (for $i, j = 1, 2$)

$$\nabla_{T_i^s} T_j^s \cdot e_t = \frac{\partial}{\partial T_i^s} \Big( (T_j \cdot e_t) \circ \pi^{-1} \Big)$$

Since $\pi$ is a local diffeomorphism, this directional derivative is the same as

$$\frac{\partial (T_j \cdot e_t)}{\partial T_i} \circ \pi^{-1}$$

Hence, the second fundamental form of $\mathcal{I}^s$ at the transitional point can be computed instead by computing at the corresponding transition point in $\mathbb{R}^5$

$$\nabla_{T_i} T_j \cdot e_t.$$

Therefore, by Eq. (7),

$$\begin{aligned} \nabla_{T_i^s} T_j^s \cdot e_t = \nabla_{T_i} T_j \cdot e_t = \nabla_{T_i} (T_j \cdot e_t) = \nabla_{T_i} \mathscr{T}^{j\hat{1}\hat{2}} \\ = \mathscr{T}^{\hat{1}\hat{2}\delta} \, \frac{\partial \mathscr{T}^{j\hat{1}\hat{2}}}{\partial s_i} + \mathscr{T}^{i\hat{2}\delta} \, \frac{\partial \mathscr{T}^{j\hat{1}\hat{2}}}{\partial \hat{s}_1} - \mathscr{T}^{i\hat{1}\delta} \, \frac{\partial \mathscr{T}^{j\hat{1}\hat{2}}}{\partial \hat{s}_2}. \end{aligned}$$

Introducing the following notations ($i, j, k \in \{1, 2\}$),

$$\mathscr{T}^{j_i\hat{1}\hat{2}} = [\frac{\partial \sigma_j}{\partial s_i} \;\; \hat{\sigma}_1 \;\; \hat{\sigma}_2], \quad \mathscr{T}^{i\hat{1}_k\hat{2}} = [\sigma_i \;\; \frac{\partial \hat{\sigma}_1}{\partial \hat{s}_k} \;\; \hat{\sigma}_2], \quad \mathscr{T}^{i\hat{1}\hat{2}_k} = [\sigma_i \;\; \hat{\sigma}_1 \;\; \frac{\hat{\sigma}_2}{\partial \hat{s}_k}]$$

yields,

$$\nabla_{T_i^s} T_j^s \cdot e_t = \; \mathscr{T}^{\hat{1}\hat{2}\delta} \; \mathscr{T}^{j_i\hat{1}\hat{2}} + \mathscr{T}^{i\hat{2}\delta} \; (\mathscr{T}^{j\hat{1}_1\hat{2}} + \mathscr{T}^{j\hat{1}\hat{2}_1}) - \mathscr{T}^{i\hat{1}\delta} \; (\mathscr{T}^{j\hat{1}_2\hat{2}} + \mathscr{T}^{j\hat{1}\hat{2}_2}).$$

Throughout this paper, we make the generic assumption that the transition point is non-degenerate, i.e., $det(\mathcal{L}) \neq 0$.

### *4.2.3 Heuristically Uniform Sampling of Local Height Contours*

To compute various transition events, the height contour curves of the local osculating quadric needs to be uniformly sampled in the *euclidean space* $\mathbb{R}^3$.

Suppose we are sampling the height contour with the time deviation $\delta t$. By Eq. (11), the sample point $p_v \in \mathbf{TS}_{\mathcal{I}^s}$ along a direction $v \in \mathbf{TS}_{\mathcal{I}^s}$, is $p_v = \sqrt{\frac{2\delta t}{II(v,v)}}\, v$. Therefore, given an initial list of sample *directions*, the following algorithm generates a list of heuristically uniform sample points.

**Algorithm 1** Heuristically Uniform Sampling

*(1) Turn the given list of sample* directions *into a list of sample* points *by scaling each element p by* $\sqrt{\frac{2\delta t}{II(p,p)}}$.
*(2) In the current list, find a neighboring sample pair* $p, q \in \mathbf{TS}_{\mathcal{I}^s}$ *with maximal distance.*
*(3) Let* $m = \frac{p+q}{2}$, *scale m by* $\sqrt{\frac{2\delta t}{II(m,m)}}$, *and insert it into the list in between p and q.*
*(4) If not enough sample points, or the distances are not approximately uniform, goto* **Step 2**.

### *4.2.4 Compute Transition Events*

**4.2.4.1 Compute Creation Events:** If $det(\mathcal{L}) > 0$ (or equivalently, the Gaussian curvature of $\mathcal{I}^s$ is positive), the osculating quadric (Eq. (11)) is an elliptic paraboloid, and the transition point has elliptic type. See Fig. 4(a).

For an upward elliptic type and offset surfaces deforming forward, or for a downward elliptic type and offset surfaces deforming backward, a creation

event is occurring, i.e., an entirely new intersection loop is created from nothing. The following algorithm computes the intersection loop at the time deviation $\delta t$ from the transition point.

**Algorithm 2** Compute Ellipse Contour for a Creation Event

*(1) Put directions* $(1,0),(0,1),(-1,0)$ *into the ordered list of directions* $\mathcal{V}$ .
*(2) Apply Algorithm. 1 to transform* $\mathcal{V}$ *to a ordered list of uniform samples in* $\mathbf{TS}_{\mathcal{I}^s}$.
*(3) Except the first and the last ones, copy and negate in order all elements, in* $\mathcal{V}$*, and append to itself.*
*(4) Map* $\mathcal{V}$ *to a ordered list of samples in* $\mathbb{R}^4_{\{s,\hat{s},t\}}$ *(cf. Observation 1).*

**4.2.4.2 Compute Annihilation Events:** At an upward elliptic transition point when offset surfaces deform backward (in time), or at a downward elliptic transition point when offset surfaces deforming forward, there is an *annihilation event* happening, i.e. an intersection loop collapses and disappears. See Fig. 4(a). The key issue here is to choose the right current intersection loop to annihilate. If there is currently only one intersection loop, annihilate it. Otherwise, we use an "evolve-to-annihilate" strategy as illustrated in Fig. 5. First, evolve all intersection loops at time $t_1$ to the time $t_1'$ (i.e., the contour position used for the pre-computation of the corresponding creation event). Then, using the inclusion test [30], find the one that the critical point $p$ identifies to annihilate.

Fig. 5 illustrates why this "evolve-to-annihilate" strategy is necessary in the simpler scenario of dynamic curve/curve intersection. Given the type of the elliptic critical point at $p$, we are sure that when deforming from the current time $t_1$ to next sampling point of time $t_2$, there must be a pair of intersection points to annihilate. However, had the inclusion test been preformed at the current time $t_1$, the right side pair of intersection points (colored in cyan) would be wrongly reported to be surrounding the considered critical point $p$ in the corresponding tangent space (tangent line for the curve/curve intersection case) and thus would wrongly selected to annihilate. This error is due to the fact that at $t_1$, the osculating paraboloid is not a good approximation to the local shape at $p$, and can be avoided if the inclusion test is applied at time $t_1'$ where the approximation is quite good and consequently the left side pair of intersection points now surrounds $p$ while the original right side pair has evolved far away from $p$.

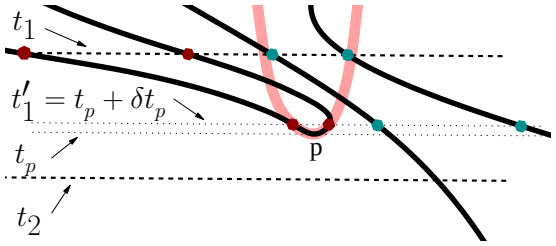


Fig. 5. **Evolve to Annihilate**

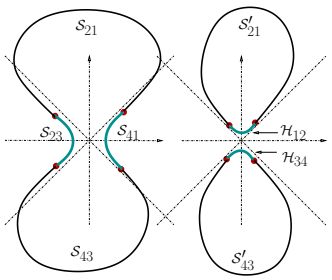


Fig. 6. **Split/Merge**

**4.2.4.3 Compute Switch Events:** If $det(\mathcal{L}) < 0$ (or equivalently, the Gaussian curvature of $\mathcal{I}^s$ is negative), the osculating quadric (Eq. (11)) is a hyperbolic paraboloid, and the transition point has hyperbolic type. See Fig. 4(b).

Deforming across a hyperbolic transition point is a quite different situation from an elliptic point inasmuch as there is a switch of two pairs of hyperbolic-like segments (cf. Fig. 3 in the euclidean space, and Fig. 4 of $\mathcal{I}^s$): 2 local segments approach each other, say, from *above* the transition point $p$ , touch *at* $p$, and then swap and depart into another two local segments *below* $p$. If the approaching pair of segments is from one intersection loop (Fig. 6), we have a split event; and if it is from 2 intersection loops (Fig. 6 in reverse order), we have a merge event. Each segment is a height contour of the local shape approximated by the osculating hyperbolic paraboloid. The following algorithm computes one pair of such height contours.

**Algorithm 3** Compute Hyperbolic Contours for a Switch Event

*(1) Put directions* $u_1 + (u_2 - u_1) * \lambda, u_1 + u_2, u_2 + (u_1 - u_2) * \lambda$ *into the ordered list of directions* $\mathcal{V}$.
*(2) Invoke Algorithm 1 to transform* $\mathcal{V}$ *to an ordered list of uniform samples in* $\mathbf{TS}_{\mathcal{I}^s}$.
*(3) In order, copy and negate all elements into another list* $\mathcal{V}'$.
*(4) Map* $\mathcal{V}$ *to an ordered list of samples in* $\mathbb{R}^4_{\{s,\hat{s},t\}}$ *(cf. Observation 1). Do the same for* $\mathcal{V}'$.

In the algorithm, $u_1$ and $u_2$ are the two asymptotic directions, which can be solved (for $u$) from the equation $II(u, u) = 0$ using the second fundamental form in Eq. (10). The algorithm also uses some coefficient $\lambda$ that is close to yet less than 1.0 so that neither of the two asymptotic direction $u_1$ and $u_2$ are sampled, because, after all, the projection of any non-zero contour can intersect neither of the two asymptotic direction where $II(u_1, u_1) = II(u_1, u_1) = 0$ (cf. Eq. (11)). The other pair of contours, with the opposite height value, can be sampled similarly, with one of the asymptotic directions reversed.

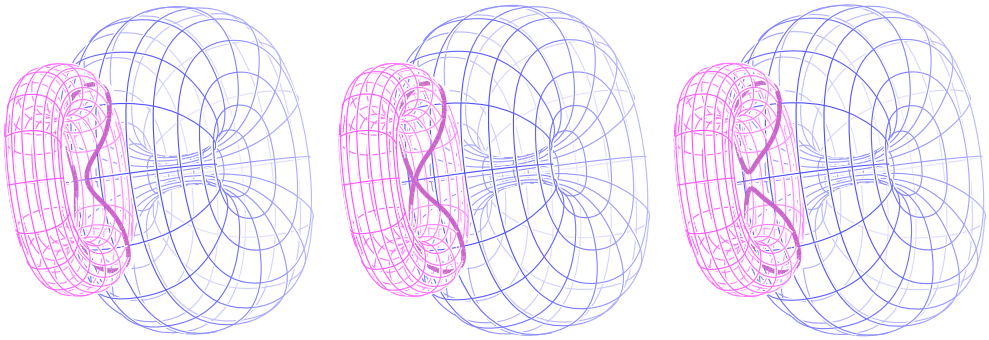

Fig. 7. **A split event of 2 deforming torus-like surfaces**

Based on the deforming direction we can determine which of the 2 principal curvature directions is the approaching direction, and which is the departing direction. Then the approaching pair of segments of current intersection curves is the one that is closest to the considered transition point along the approaching direction. Using Algorithm 3, the switch event can be computed by cutting the two approach segments, evolving the rest across, say upward, $p$, and then pasting the other pair of contours to the departing pair of segments (Illustrated Fig. 6). Finally, Fig. 7 gives an example of split event of two deforming torus-like surfaces. The images in Fig. 8 provide several snapshots showing the topological changes which occur in the intersection curves when deforming two initially flat surfaces. Fig. 8(2) shows the randomly chosen generalized offset vector field for one surface used in generating the sequence. Notice that split events and merge events in the images are classified according to, respectively, the split and merge of intersection curves rather than the regions surrounded by them. For demo videos, see http://www.cs.utah.edu/∼xchen/papers/more.html

## 5 Conclusion

In this paper, we have applied a mathematical framework provided by singularity theory to develop algorithms for continuously and robustly tracking the intersection curves of two generically deforming surfaces, on the assumption that both the base surfaces and the deforming vectors have piecewise rational representation. The core idea is to divide the process into two steps depending on when transition points occur. Away from any transition points, the intersection curves evolve without any structural change. We found a simple and robust method which constructs an evolution vector field directly in the Euclidean space $\mathbb{R}^3$ and evolves the intersection curves accordingly. A method is developed for identifying transition points and following topological changes in the intersection curves by introducing an implicit 2-manifold $\mathcal{I}$, formed by the union of intersection curves in an augmented parameter space. The transition points are identified as the points on $\mathcal{I}$ where the tangent spaces are

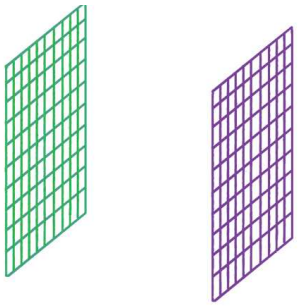

(1) initial flat surfaces

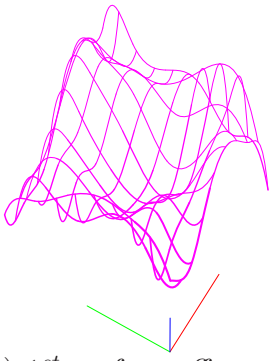

(2) $1^{st}$ surface offset vector

(3) 4 loops created

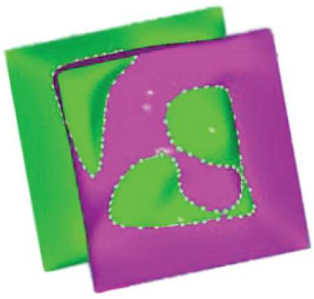

(4) 2 merge events

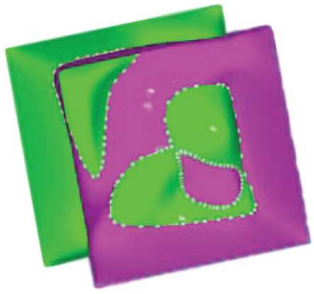

(5) a split event

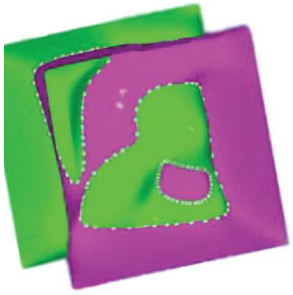

(6) no transition event

(7) a merge event

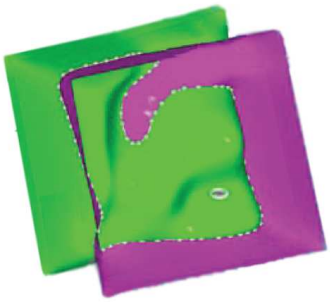

(8) no transition event

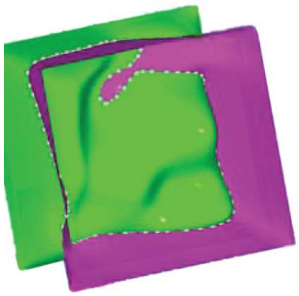

(9) a loop annihilated

(10) a split event

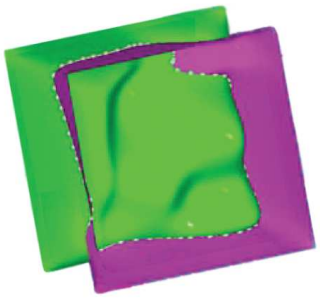

(11) another annihilation

Fig. 8. **Series of transitions for intersection curves of deforming surfaces**

orthogonal to $t$-axis, and the topological change of the intersection curves is subsequently computed by 2nd order differential geometric computations on $\mathcal{I}$.

Singularity theory, on which this approach is based, assumes the transition points are generic; that is, they are isolated and satisfy robustness and stability conditions. Thus, a plane and a cylinder whose axis is parallel to the plane touch non-generically in a line of contact points before evolving into a well defined intersection curve. Cases such as this are not covered by the presented approach.

There are also further transitions which can occur for deforming surfaces, including the surface developing singularities, self-intersections, and triple intersection points. We are now developing a similar formulation for tracking the intersection curve end points that correspond to surface boundaries, and for tracking triple intersection points.

## References


[1] J. Mather *Stability of $C^\infty$–mappings*, *I: The Division Theorem* Ann. of Math **89** (1969) 89–104; *II. Infinitesimal stability implies stability*, Ann. of Math. **89** (1969) 254–291; *III. Finitely determined map germs* , Inst. Hautes Etudes Sci. Publ. Math. **36** (1968) 127–156; *IV. Classification of stable germs by $\mathbb{R}$–algebras* , Inst. Hautes Etudes Sci. Publ. Math. **37** (1969) 223–248; *V. Transversality* , Adv. in Math. **37** (1970) 301–336; *VI. The nice dimensions* , Liverpool Singularities Symposium I , Springer Lecture Notes in Math. **192** (1970) 207–253

[2] K. Abdel-Malek and H. Yeh, "Determining intersection curves between surfaces of two solids," *Computer-Aided Design*, vol. 28, no. 6-7, June-July 1996, pp. 539–549.

[3] C. L. Bajaj, C. M. Hoffmann, R. E. Lynch, and J. E. H. Hopcroft, "Tracing surface intersections," *Computer Aided Geometric Design*, vol. 5, no. 4, November 1988, pp. 285–307.

[4] R. E. Barnhill, G. Farin, M. Jordan, and B. R. Piper, "Surface/surface intersection," *Computer Aided Geometric Design*, vol. 4, no. 1-2, July 1987, pp. 3–16.

[5] R. E. Barnhill and S. N. Kersey, "A marching method for parametric surface/surface intersection," *Computer Aided Geometric Design*, vol. 7, no. 1-4, June 1990, pp. 257–280.

[6] J. Damon, "On the Smoothness and Geometry of Boundaries Associated to Skeletal Structures I: Sufficient Conditions for Smoothness," *Annales Inst. Fourier*, vol. 53, 2003, pp. 1941–1985.

[7] J. Damon, "On the Smoothness and Geometry of Boundaries Associated

to Skeletal Structures II: Geometry in the Blum Case," *Compositio Mathematica*, vol. 140, no. 6, 2004, pp. 1657–1674.

[8] J. Damon, "Determining the Geometry of Boundaries of Objects from Medial Data," *Int. Jour. Comp. Vision*, vol. 63, no. 1, 2005, pp. 45–64.

[9] G. Elber and E. Cohen, "Error bounded variable distance offset operator for free form curves and surfaces," *Int. J. Comput. Geometry Appl*, vol. 1, no. 1, 1991, pp. 67–78.

[10] G. Elber and M.-S. Kim, "Geometric constraint solver using multivariate rational spline functions," *ACM Symposium on Solid Modeling and Applications*, 2001, pp. 1–10.

[11] G. Elber, I.-K. Lee, and M.-S. Kim, "Comparing offset curve approximation methods," *IEEE Computer Graphics and Applications*, vol. 17, 1997, pp. 62–71.

[12] R. T. Farouki and C. A. Neff, "Analytic properties of plane offset curves," *Computer Aided Geometric Design*, vol. 7, no. 1-4, 1990, pp. 83–99.

[13] R. Goldman, "Curvature formulas for implicit curves and surfaces," *Computer Aided Geometric Design*, vol. 22, no. 7, 2005, pp. 632–658.

[14] B. Hamann, "Visualization and Modeling Contours of Trivariate Functions, Ph.D. thesis," *Computer Science Department, Arizona State Univeristy*, 1991.

[15] M. E. Hohmeyer, "A surface intersection algorithm based on loop detection," *Proceedings of the first ACM symposium on Solid modeling foundations and CAD/CAM applications*. May 1991, pp. 197–207, ACM Press.

[16] C. Y. Hu, T. Maekawa, N. M. Patrikalakis, and X. Ye, "Robust Interval Algorithm for Surface Intersections," *Computer-Aided Design*, vol. 29, no. 9, September 1997, pp. 617–627.

[17] C.-S. Jun, D.-S. Kim, D.-S. Kim, H.-C. Lee, J. Hwang, and Tien-ChienChang, "Surface slicing algorithm based on topology transition," *Computer-Aided Design*, vol. 33, no. 11, September 2001, pp. 825–838.

[18] R. Kimmel and A. M. Bruckstein, "Shape offsets via level sets," *Computer-Aided Design*, vol. 25, no. 3, March 1993, pp. 154–162.

[19] J. J. Koenderink, *Solid Shape*, MIT press, 1990.

[20] G. A. Kriezis, N. M. Patrikalakis, and F. E. Wolter, "Topological and differential-equation methods for surface intersections," *Computer-Aided Design*, vol. 24, no. 1, January 1992, pp. 41–55.

[21] G. V. V. R. Kumar, K. G. Shastry, and B. G. Prakash, "Computing offsets of trimmed NURBS surfaces," *Computer-Aided Design*, vol. 35, no. 5, April 2003, pp. 411–420.

[22] S. Lang, *Undergraduate Analysis*, 2 edition, Springer, 1997.

[23] T. Maekawa, "An overview of offset curves and surfaces," *Computer-Aided Design*, vol. 31, no. 3, March 1999, pp. 165–173.

[24] T. Maekawa and N. M. Patrikalakis, "Computation of singularities and intersections of offsets of planar curves.," *Computer Aided Geometric Design*, vol. 10, no. 5, 1993, pp. 407–429.

[25] R. P. Markot and R. L. Magedson, "Solutions of tangential surface and

curve intersections," *Computer-Aided Design*, vol. 21, no. 7, September 1989, pp. 421–427.

[26] B. O'Neill, *Elementary Differential Geometry*, 2 edition, Academic Press, 1997.

[27] Y. Ouyang, M. Tang, J. Lin, and J. Dong, "Intersection of two offset parametric surfaces based on topology analysis," *Journal of Zhejiang Univ SCI*, vol. 5, no. 3, 2004, pp. 259–268.

[28] N. M. Patrikalakis, T. Maekawa, K. H. Ko, and H. Mukundan, "Surface to Surface Intersections," *Computer-Aided Design and Applications*, vol. 1, no. 1-4, 2004, pp. 449–458.

[29] B. Pham, "Offset curves and surfaces: a brief survey," *Computer-Aided Design*, vol. 24, no. 4, April 1992, pp. 223–229.

[30] F. P. Preparata and M. I. Shamos, *Computational geometry: an introduction*, Springer-Verlag, 1985.

[31] T. W. Sederberg, H. N. Christiansen, and S. Katz, "Improved test for closed loops in surface intersections," *Computer-Aided Design*, vol. 21, no. 8, October 1989, pp. 505–508.

[32] T. W. Sederberg and R. J. Meyers, "Loop detection in surface patch intersections," *Computer Aided Geometric Design*, vol. 5, no. 2, July 1988, pp. 161–171.

[33] E. C. Sherbrooke and N. M. Patrikalakis, "Computation of the solutions of nonlinear polynomial systems," *Computer Aided Geometric Design*, vol. 10, no. 5, 1993, pp. 379–405.

[34] T. S. Smith, R. T. Farouki, M. al Kandari, and H. Pottmann, "Optimal slicing of free-form surfaces," *Computer Aided Geometric Design*, vol. 19, no. 1, Jan. 2002, pp. 43–64.

[35] O. Soldea, G. Elber, and E. Rivlin, "Global Curvature Analysis and Segmentation of Volumetric Data Sets using Trivariate B-spline Functions," *Geometric Modeling and Processing 2004*, April 2004, pp. 217–226.

[36] J.-P. Thirion and A. Gourdon, "Computing the Differential Characteristics of Isointensity Surfaces," *Journal of Computer Vision and Image Understanding*, vol. 61, no. 2, March 1995, pp. 190–202.

[37] J. Wallner, T. Sakkalis, T. Maekawa, H. Pottmann, and G. Yu, "Self-Intersections of Offset Curves and Surfaces," *International Journal of Shape Modelling*, vol. 7, no. 1, June 2001, pp. 1–21.

[38] G. Xu and C. L. Bajaj, "Curvature Computations of 2-Manifolds in $\mathbb{R}^k$," *J. Comp. Math.*, vol. 21, no. 5, 2003, pp. 681–688.

[39] X. Ye and T. Maekawa, "Differential Geometry of Intersection Curves of Two Surfaces," *Computer Aided Geometric Design*, vol. 16, no. 8, September 1999, pp. 767–788.